Available online at www.sciencedirect.com
ScienceDirect
International Journal of Thermal Sciences 48 (2009) 825–836
International Journal of Thermal Sciences
www.elsevier.com/locate/ijts

Modelling of improved energy performance of air-cooled chillers with mist pre-cooling

F.W. Yu *, K.T. Chan

Department of Building Services Engineering, The Hong Kong Polytechnic University, Hung Hom, Hong Kong, China

Received 28 February 2008; received in revised form 16 April 2008; accepted 9 June 2008

Available online 19 August 2008

Abstract

Air-cooled chillers are widely used to provide cooling energy and yet pragmatic and simple energy efficient measures for them are still lacking. This paper considers how their coefficient of performance (COP) can be improved by using mist to pre-cool ambient air entering the condensers. The benefit of this application rests on the decrease of compressor power resulting from the reduced condenser air temperature with insignificant consumption of water and pump power associated with the mist generation. Based on a simulation analysis of an air-cooled screw chiller operating under head pressure control, applying such mist pre-cooling enables the COP to increase by up to 7.7%. Precise control of mist generation rate and integration with floating condensing temperature control are the major challenges of using a mist system to maximize electricity savings. The results of this study will prompt low-energy operation of existing air-cooled chillers working for various climatic conditions.

Keywords: Air-cooled chiller; Coefficient of performance; Electricity consumption; Water mist

1. Introduction

Air-cooled chillers are an inevitable choice for central cooling systems in buildings whenever fresh water is considered to be a precious resource which cannot be used freely for evaporative cooling towers in the heat rejection process. They may even be a preferable choice for most small to medium scale buildings due to the ease of installation, the simplicity of operation and maintenance, and the lower installation and maintenance costs as compared to water-cooled chillers. Yet concern has been expressed about the considerable electricity consumed by these chillers when in use because they are recognized as "less-efficient" equipment compared with water-cooled chillers.

According to many studies [1–8], the deficient performance of air-cooled chillers is mainly due to head pressure control (HPC) under which the condensing temperature floats around a high set point of 50 °C based on a design outdoor temperature of 35 °C, irrespective of different chiller loads and weather conditions. The condenser fan power under HPC can be kept low but with considerable compressor power at such high condensing temperature. To overcome this, proper control of condensing temperature should be developed to optimize the trade-off between the compressor power and condenser fan power, given that the condensing temperature can vary widely in response to outdoor temperatures ranging between 10 to 35 °C. Floating condensing temperature control (CTC) is proposed as an alternative to HPC to lower the condensing temperature in response to changes of ambient and load conditions [6–8]. The condenser fans under CTC are staged as many as possible in most operating conditions to enhance the heat rejection airflow required to decrease the condensing temperature. Simulation analyses on air-cooled screw or centrifugal chillers [7,8] confirmed that the coefficient of performance (COP) of the chillers could increase by up to 237.2% when variable speed condenser fans are used to complement CTC. A COP is defined as the chiller load in kW divided by the power input in kW. The variable speed fans are capable of modulating smoothly the heat rejection airflow with reduced power while enhancing the controllability of condensing temperature. To implement CTC, the set point of condensing temperature should be adjusted in response to variations of outdoor temperature and chiller part load ratios. Although the idea of CTC is easily recognized and there should

* Corresponding author. Tel.: +852 37460416; fax: +852 23647375.
E-mail address: ccyufw@hkcc-polyu.edu.hk (F.W. Yu).

1290-0729/$ – see front matter
doi:10.1016/j.ijthermalsci.2008.06.016

Nomenclature

CAPFT	regression function for chiller capacity
COP	chiller coefficient of performance
CTC	floating condensing temperature control
C_{pa}	specific heat capacity of air, assumed to be 1.02 kJ/(kg °C)
C_{pw}	specific heat capacity of water, assumed to be 4.19 kJ/(kg °C)
E	power input ..... kW
EIRFT	regression function for compressor efficiency
EIRFPLR	regression function for compressor efficiency at part load conditions
Eff_{cd}	condenser heat transfer effectiveness
h_{db}	specific enthalpy with dry bulb temperature ... °C
HPC	head pressure control
m_{mist}	mist generation rate ..... kg/s or l/s
m_w	mass flow rate of chilled water ..... kg/s or l/s
PLR	chiller part load ratio
RH	relative humidity ..... %
Q_{cd}	heat rejection ..... kW
Q_{cl}	chiller load ..... kW
T_{cd}	condensing temperature ..... °C
T_{cdae}	temperature of air entering the condenser ..... °C
T_{cdal}	temperature of air leaving the condenser ..... °C
T_{chwr}	temperature of return chilled water ..... °C
T_{chws}	temperature of supply chilled water ..... °C
T_{db}	dry bulb temperature ..... °C
T'_{db}	reduced temperature from dry bulb temperature with mist pre-cooling ..... °C
T_{wb}	wet bulb temperature ..... °C
T_{ev}	evaporating temperature ..... °C
V_a	airflow provided by the staged condenser fans ..... m^3/s
W_{db}	moisture content with dry bulb temperature ..... kg/kg dry air
W'_{db}	increased moisture content from W_{db} ..... kg/kg dry air
ρ_a	air density, assumed to be 1.2 kg/m^3

Subscripts

cc	compressor
ch	chiller
cd	condenser
cf	condenser fan
rated	at rated conditions

be no technical difficulty in implementing the condensing temperature reset, chiller manufacturers seem to be reluctant to commercialize CTC with variable speed condenser fans operating at optimum condensing temperatures in order to maximize the COP of air-cooled chillers.

Evaporative cooling of ambient air is not a new concept for air-conditioning systems, but its application on pre-cooling air entering air-cooled condensers is not common. As some studies indicated [9,10], evaporative pre-coolers, when installed in front of air-cooled condensers, can pre-cool outdoor air before entering the condensers while consuming less than 15% of the cooling water required by cooling towers and evaporative condensers. For an evaporative pre-cooler, hot air flows across a porous wetted surface with a film of cool water. That air absorbs and evaporates moisture on the surface when leaving the pre-cooler, and then its dry bulb temperature drops and approaches its wet bulb temperature. The pre-coolers enable the condensing temperature to drop in response to a reduction in outdoor temperature. However, the pressure drop across the pre-coolers incurs additional fan power. Another power will be taken up by a small pump which operates to produce a low flow rate of circulating water in order to maintain the wetted surface. The potential and benefits of using evaporative pre-coolers hinge on the extent to which the condensing temperature can drop and whether the decrease in compressor power due to this drop can outweigh the pump power in addition to the fan power. Zhang et al. [9] have indicated that the use of evaporative pre-coolers can bring about a 14.7% increase in the COP of air-cooled chillers working in a hot and dry environment. According to a simulation study [11], a 1.4–14.4% decrease in chiller power and a 1.3–4.6% increase in the refrigeration effect could be achieved when an air-cooled reciprocating chiller with an evaporative pre-cooler operated under HPC. When CTC replaced HPC, the chiller power could be further reduced by 1.3–4.3% in certain operating conditions. The pre-coolers are expected to have high effectiveness when cooling outdoor air in a hot and dry climate, but they can function properly even when the climate is hot and humid [11].

Apart from installing an evaporative pre-cooler in front of an air-cooled condenser, the evaporative cooling of ambient air can be done more directly via a water mist cooling system. The system produces a cloud of very fine water droplets via atomization nozzles, which allows the ambient air entering the condenser to cool from its dry bulb temperature to wet bulb temperature while the droplets are fully vaporized. The system does not cause any flow resistance to the air stream and therefore no additional fan power will be incurred. It takes up only a small amount of electric power to drive the high pressure pump and negligible amount of water for mist generation. Yet there is a lack of research into how to reap the benefits of such mist pre-cooling for air-cooled chillers.

The aim of this paper is to investigate how the COP of air-cooled chillers can be improved by mist pre-cooling. First, the typical arrangement of a mist system and its use with air-cooled condensers will be explained. Second, a simulation analysis will be made on how a mist system should operate with an air-cooled screw chiller and the subsequent change in part load performance under various load and ambient conditions. Following that, the cooling load profile of an institutional building will be considered to identify electricity savings of the chillers

with mist pre-cooling. Challenges of taking a definite advantage for the chillers with mist pre-cooling will be discussed. The significance of this study is to present a possible scheme to make the operation of air-cooled chillers more sustainable.

2. Description of mist system and pre-cooling of condenser air

Fig. 1 shows a schematic diagram of a water mist installation, which contains basically atomization nozzles, water pipework, a filter assembly and a high pressure pump. An UV lamp may be inserted before the filters to disinfect ordinary water for mist generation. When the constant speed pump operates to deliver water through the pipework at a high pressure of around 70 bars, the water is released through the low flow atomization nozzles to form a mist of very fine droplets in 10-micron size. These droplets can be easily vaporized by ambient air before entering the condenser and a reduction in the temperature of that air follows the adiabatic cooling process with constant specific enthalpy.

Depending on the layout of the condenser coil, the nozzles should be evenly distributed in front of the entire condenser surface in order to ensure that all the air entering the condenser can be pre-cooled by vaporizing the mist. Fig. 2 shows an example of pipe and nozzle layouts for an existing air-cooled screw chiller. A distance of 500 to 750 mm should be maintained between the nozzles and the condenser in order to prevent the mist which the air stream carries from falling on the condenser fins and coil without undergoing the vaporization process.

The number of nozzles, water circuits and pump sets depends on how much mist is required to generate and how the mist system operates with the chiller. Each refrigeration circuit within a chiller should be designed with an individual mist installation in order to avoid unnecessary mist generation when some of the refrigeration circuits are idle while the chiller is operating at partial load conditions. The design outdoor conditions and the total heat rejection airflow rate of a chiller are the two major parameters for determining the peak mist generation rate required. Regarding the local design conditions of 35 °C dry bulb and relative humidity (RH) of 70%, the moisture content required to cool the air adiabatically at 90% RH is 0.0015 kg/kg of dry air. For a given total heat rejection airflow rate ($V_{a,rated}$), the peak mist generation rate will be $(0.0015 \times V_{a,rated} \times \rho_a)$ kg/s. Based on the mist generation rate calculated, the number of nozzles required and the pump power rating can be decided according to the specifications given by system suppliers.

Given a fixed mist generation rate, the extent to which the dry bulb temperature can drop depends on load and ambient conditions and on how the heat rejection airflow varies to maintain the condensing temperature at its set point under various operating conditions. The following section will report a detailed analysis on how mist pre-cooling influences the COP of an existing air-cooled chiller and on what parameter should be considered to optimize the control and operation of the mist system with the chiller.

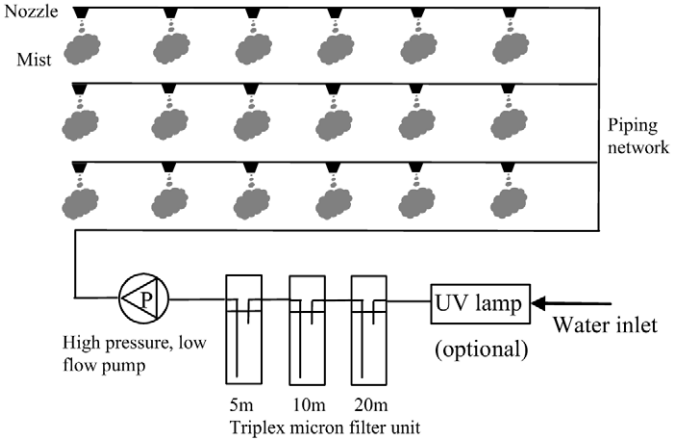

Fig. 1. Typical water mist installation.

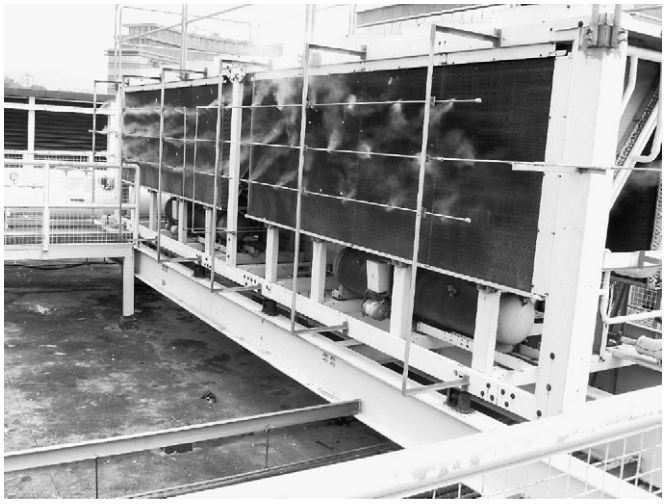

Fig. 2. A picture showing pipe and nozzle layouts of a mist system for the condenser of an air-cooled chiller.

3. Example of applying mist pre-cooling to air-cooled chiller

3.1. Description of the chiller and its mist installations

The air-cooled chiller equipped with a water mist system (as shown in Fig. 2) is based on one of the five chillers operating for an institutional building. It has a nominal capacity of 1152 kW and a COP of 2.8 at full load with an outdoor temperature of 35 °C. The power input for calculating that COP includes the compressor power, condenser fan power and control circuit power. The chiller uses the refrigerant R134a and has two identical refrigeration circuits, each of which contains two screw compressors. The shell-and-tube flooded type evaporator is designed to produce chilled water at a constant flow rate of 50 kg/s with supply and return temperatures of 7 and 12.5 °C, respectively. The cooling output is modulated from 15 to 100% in steps via adjusting the number of compressors operating and their sliding valve positions while controlling the temperature of supply chilled water at a set point of 7 °C. Each refrigeration circuit is equipped with an electronic expansion valve to main-

tain proper level of the refrigerant in the evaporator when the chiller load varies.

The heat rejection capacity of the air-cooled condenser is designed to control the condensing temperature (T_{cd}) at around 50 °C when the temperature of air entering the condenser (T_{cdae}) is 35 °C. Under this design condition, the heat transfer effectiveness of the condenser (Eff_{cd}), defined by $(T_{cdal} - T_{cdae})/(T_{cd} - T_{cdae})$, was identified to be 0.8, where T_{cdal} is the temperature of air leaving the condenser. The number of staged condenser fans is based on the heat rejection airflow required to maintain the condensing temperature at its set point under HPC. The air-cooled condenser contains 16 identical condenser fans to deliver a total airflow rate of 85.52 m^3/s. The fans are divided into eight groups and each refrigeration circuit operates with four fan groups. Under this arrangement, heat rejection airflow is regulated from 10.69 through 85.52 m^3/s in eight steps, depending on the ambient and load conditions. Each fan is of the high static type with a power rating of 4.1 kW and the total fan power is 65.6 kW when all the fans are operating.

The measured variables of the chiller included the percentage load, temperatures of supply and return chilled water (T_{chws} and T_{chwr}), power of each compressor (E_{cc}) and each refrigeration circuit (E_{ch}), evaporating temperature (T_{ev}) and condensing temperature (T_{cd}) of each refrigeration circuit. They were monitored and logged at 15-min intervals by a building management system. Readings of the percentage load were taken from the chiller microprocessor which controlled the capacity step required to maintain T_{chws} within the dead band of 1 °C from its set point at various cooling loads. Resistance type temperature sensors were used to measure the temperature variables at an uncertainty of ±0.1 °C of readings. Regarding the measurements of T_{chwr} and T_{chws}, the probes of the sensors were immersed in the chilled water flowing through the evaporator's inlet and outlet. There was no meter to measure directly the chilled water flow rate (m_w) but an estimation of the actual value was made based on the monitored differential pressure across the constant speed pump dedicated to the chiller and the pressure-flow characteristics of the pump. For many operating conditions m_w was found to comply with its nominal value of 50 kg/s. The chiller load (Q_{cl}), computed by $m_w C_{pw}(T_{chwr} - T_{chws})$, was determined accordingly. Considering the use of a fixed reading for m_w, the uncertainty of the calculated Q_{cl} is due to the measurement errors of T_{chwr} and T_{chws}. The percentage measurement error of T_{chws} was 1.43% at the reading of 7 °C for all operating conditions, while that of T_{chwr} was 0.8 % at the reading of 12.5 °C with full load and 1.28% at the reading of 7.83 °C with the lowest percentage load of 15%. The root sum square error of Q_{cl} due to all these measurement errors was calculated to be 1.64% with full load and 1.92% with 15% of full load.

E_{cc} and E_{ch} were metered by power analysers with an uncertainty of ±0.1 kW at the measured range of 1 to 999 kW. The analysers were located next to the switchgears serving the whole chiller unit and individual compressors and they measured the voltage, running current and power factor of each phase of the electrical circuits. The chiller COP was then computed by Q_{cl} divided by the measured E_{ch}. Regarding the chiller part load ratios ranging from 0.15 to 1, E_{ch} could vary from 48.4 to 409 kW, so its percentage measurement error could change from 0.21 to 0.024%. The root sum square error of chiller COP due to all the measurement errors of T_{chws}, T_{chwr} and E_{ch} was calculated to be 1.64% with full load and 1.93% with the 15% of full load.

An uncertainty analysis was carried out on the COP computed based on the T_{chws}, T_{chwr} and E_{ch} measured with individual uncertainties. Table 1 shows how the measurement error of each input variable (i.e. input uncertainty) influences the calculated results of chiller COP when the chiller was operating at full load and the lowest part load ratio (PLR) of 0.15. The selection of minimum and maximum perturbations is based on the possible change of each measured variable. Based on the dead band setting, T_{chws} can deviate by 1 °C from its set point of 7 °C for all operating conditions, so its minimum and maximum perturbations are 6 and 8 °C, respectively. Following the deviation of T_{chws}, the minimum and maximum perturbations of T_{chwr} are 11.5 and 13.5 °C for the base value of 12.5 °C at full load, and 6.83 and 8.83 °C for the base value of 7.83 °C at a PLR of 0.15. When T_{chws} and T_{chwr} are maintained at their base values at a given PLR, E_{ch} can vary in response to the ambient conditions. The minimum and maximum perturbations of E_{ch} are associated with an outdoor dry bulb temperature of 10 to 35 °C, respectively. The output change of chiller COP was evaluated with respect to the input change of each measured variable. The unit-bearing sensitivity coefficient, defined as the output change over input change, was then computed for each of the variables. Given the uncertainty (measurement error) of each input variable, it is possible to identify the un-

Table 1
Uncertainty analysis of operating variables

Input variable	Base case	Perturbations		Input uncertainty	Sensitivity coefficient	Uncertainty of chiller COP
		Min.	Max.			
Full load						
T_{chwr} (°C)	12.5	11.5	13.5	0.1 °C (0.8%)	0.025 $°C^{-1}$	0.0025 (0.089%)
T_{chws} (°C)	7	6	8	0.1 °C (1.43%)	0.025 $°C^{-1}$	0.0025 (0.089%)
E_{ch} (kW)	409	589.8	409	0.1 kW (0.024%)	0.010 kW^{-1}	0.0010 (0.035%)
Part load ratio of 0.15						
T_{chwr} (°C)	7.83	6.83	8.83	0.1 °C (1.28%)	0.005 $°C^{-1}$	0.0005 (0.034%)
T_{chws} (°C)	7	6	8	0.1 °C (1.43%)	0.005 $°C^{-1}$	0.0005 (0.034%)
E_{ch} (kW)	116.4	48.4	116.4	0.1 kW (0.086%)	0.031 kW^{-1}	0.0031 (0.208%)

certainty of chiller COP—the input uncertainty multiplied by sensitivity coefficient. As Table 1 illustrates, the percentage uncertainty of chiller COP due to T_{chws} or T_{chwr} is much lower than their respective percentage measurement errors. E_{ch} is the most influential parameter among the three input variables, which tends to enlarge the percentage uncertainty of chiller COP to up to 0.208% when the chiller part load ratio dropped to 0.15.

The dry bulb temperature (T_{db}) and relative humidity (RH) of ambient air were monitored along with the measured variables of the chiller. They were used to control two identical water mist installations, each with a high pressure pump rated at 0.75 kW and dedicated to one refrigeration circuit. The mist systems were designed to provide a total mist generation rate of 0.067 l/s which accounts for only 43% of 0.154 l/s computed based on the calculation of peak mist generation rate mentioned in Section 2. This suggests that the designer made a conservative estimate on the required mist generation rate in an attempt to make sure that all the mist generated are fully vaporized by the air entering the condenser without being carried over the condenser fins and coil. It is noted that the water consumption rate of 0.067 l/s is very small, compared with 0.93 l/s required for a hypothetical cooling tower serving the chiller. The calculation of 0.93 l/s is based on an assumption that the water loss accounts for 1.5% of the condenser water flow rate designed at 0.054 l/s per kW cooling capacity specified in standard rating conditions for chiller performance rating [12].

3.2. Simulation analysis of chiller COP

The performance of the chiller with and without using mist pre-cooling has to be analysed with the aid of chiller modelling in view of the absence of measured data on the heat rejection airflow and temperature of air leaving the condenser. A regression model based on DOE-2 [13] was developed to simulate the part-load and off-design COP of the chiller. The model was calibrated by using 1585 sets of the actual operating data collected from the chiller over the period of January to August 2007. This data set covers various operating conditions in terms of different combinations of dry bulb temperatures from 11.0 to 30.7 °C and chiller part load ratios (PLR) from 0.30 to 0.93. Eqs. (1) to (5) give the five regression curves used to predict compressor power (E_{cc}), given the chiller load (Q_{cl}), the temperature of air entering the condenser (T_{cdae}), chilled water supply temperature (T_{chws}), full load compressor power ($E_{cc,rated}$) and chiller nominal capacity ($Q_{cl,rated}$) at rated conditions.

$$\begin{aligned}\mathrm{CAPFT} = {} & -0.09464899 + 0.0383407 \times (1.8T_{chws} + 32) \\ & - 0.00009205 \times (1.8T_{chws} + 32)^2 \\ & + 0.00378007 \times (1.8T_{cdae} + 32) \\ & - 0.00001375 \times (1.8T_{cdae} + 32)^2 \\ & - 0.00015464 \times (1.8T_{chws} + 32) \\ & \times (1.8T_{cdae} + 32) \end{aligned} \quad (1)$$

$$\begin{aligned}\mathrm{EIRFT} = {} & 0.13545636 + 0.02292946 \times (1.8T_{chws} + 32) \\ & - 0.00016107 \times (1.8T_{chws} + 32)^2 \\ & - 0.00235396 \times (1.8T_{cdae} + 32) \\ & + 0.00012991 \times (1.8T_{cdae} + 32)^2 \\ & - 0.00018685 \times (1.8T_{chws} + 32) \\ & \times (1.8T_{cdae} + 32) \end{aligned} \quad (2)$$

$$\mathrm{PLR} = Q_{cl}/(Q_{cl,rated}\,\mathrm{CAPFT}) \quad (3)$$

$$\mathrm{EIRFPLR} = 0.0084 + 0.9615\mathrm{PLR} + 0.0706\mathrm{PLR}^2 \quad (4)$$

$$E_{cc} = E_{cc,rated} \times \mathrm{CAPFT} \times \mathrm{EIRFT} \times \mathrm{EIRFPLR} \quad (5)$$

The two adjustment factors (CAPFT and EIRFT) for full load conditions with variations in T_{chws} and T_{cdae} are based on the default equations used in DOE-2. The adjustment factor (i.e. Eq. (4)) for compressor efficiency at part load operation was the best-fit regression curve with the coefficient of determination (R^2) of 0.89 based on the correlation between the EIRFPLR and PLR calculated by the measured data. The accuracy of the chiller model was examined by comparing the COP (expressed here as Q_{cl}/E_{cc}) calculated directly by the measured data with that predicted by Eqs. (1) to (5). The mean bias error (MBE) and root mean square error (RMSE) were used to quantify the difference between the predicted and actual COP. They were determined to be 0.0733 (1.77% of the mean COP of 2.83) and 0.3475 (8.38% of the mean COP of 2.83), respectively. The smaller value of MBE may be due to the mutual cancellation between over-estimation and under-estimation among the predicted results of the COP. Both the MBE and RMSE normalized by the mean COP are well below 10%, suggesting that the regression model is fairly accurate in the prediction of COP.

Heat rejection (Q_{cd}) was calculated directly by using Eq. (6). The variation of the condensing temperature (T_{cd}) at part load conditions could be expressed by Eq. (7), based on a plot of the measured T_{cd} against the PLR calculated by the measured data. Given Eq. (7), it is possible to evaluate the effective heat rejection airflow (V_a) by Eq. (8), where the heat transfer effectiveness of the condenser (Eff_{cd}) of 0.8 identified at full load was used for all operating conditions. The total condenser fan power was determined by using Eq. (9), considering that the airflow is directly proportional to the power of a fan running at constant speed.

$$Q_{cd} = Q_{cl} + E_{cc} \quad (6)$$

$$T_{cd} = 34.982 + 0.1493\mathrm{PLR} + 16.087\mathrm{PLR}^2 \quad (7)$$

$$V_a = \frac{Q_{cd}}{\rho_a C_{pa} Eff_{cd}(T_{cd} - T_{cdae})} \quad (8)$$

$$E_{cf} = E_{cf,rated} V_a / V_{a,rated} \quad (9)$$

In the absence of mist pre-cooling, T_{cdae} is simply equal to the ambient dry bulb temperature (T_{db}) which is independent of V_a, so all the equations can be solved directly based on the given inputs. While the mist system operates, T_{cdae} refers to the temperature (T'_{db}) reduced from T_{db}, of which the increased moisture content W'_{db} is dependent on V_a and the mist generation rate (m_{mist}). Their relationship is given by Eqs. (10) to (12). The validity of Eq. (10) is based on an assumption that no

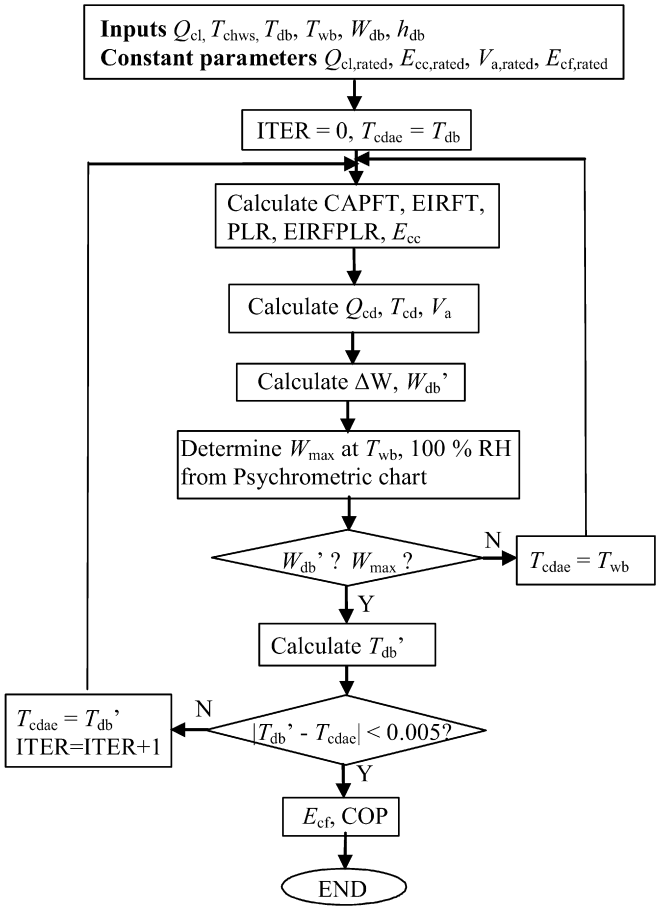

Fig. 3. Procedure for evaluating operating variables of the chiller with mist pre-cooling.

mist is lost to the surroundings. In cases where the calculated W'_{db} is greater than the maximum allowable moisture content at the saturation state (i.e. T_{wb} at 100% RH), T'_{db} becomes T_{wb} and the surplus mist may be carried over the condenser coil.

$$\Delta W = m_{mist}/(V_a \rho_a) \tag{10}$$

$$W'_{db} = W_{db} + \Delta W \tag{11}$$

$$T'_{db} = (h_{db} - 2501 W'_{db})/(1.006 + 1.805 W'_{db}) \tag{12}$$

Due to the interdependence of the variables in the presence of mist pre-cooling, the whole set of Eqs. (1) to (12) has to be solved through an iterative process shown in Fig. 3. For any given inputs, T_{db} was taken to be the initial value of T_{cdae}. All variables were determined by using Eqs. (1) through (12). If the difference between the T'_{db} and T_{cdae} was less than a specified tolerance of ±0.005 °C, all the variables calculated were convergent to their own values with the required accuracy. Otherwise iterations were performed by replacing T_{cdae} with T'_{db} in order to meet the convergent criterion.

3.3. Part load performance of the chiller with mist pre-cooling

Drawing on the chiller model, the influence of mist pre-cooling on the chiller COP was investigated with respect to a complete set of 21481 operating conditions for the period of January to August 2007 with various combinations of chiller loads (PLR from 0.1 to 1), dry bulb temperatures (T_{db} from 9.4 to 36 °C) and relative humidity (RH from 37.3 to 100%). In this part, the COP calculation is based on the overall power input to the compressors, condenser fans and high pressure pumps when operating. Based on the frequency distribution shown in Table 2, there is no clear correlation between RH and T_{db} under the local subtropical climate. RH exceeds 80% for 58.1% of the total operating time and T_{db} of above 28 °C accounts for 25.8% of the total operating time. If the mist system operates based on the supplier's recommendation ($T_{db} > 28$ °C at RH < 77%), mist pre-cooling will take effect for only 11.4% of the total operating time.

Figs. 4 and 5 show the simulation results of the percentage change of COP from baseline (without mist pre-cooling) with respect to different weather parameters, when the chiller operated at part load ratios (PLRs) of 0.5–0.6 (with 2645 data sets) and of 0.9–1 (with 3160 data sets). The wide spread of the percentage change of COP is mainly due to various combinations of the weather parameters with the PLRs. A change of chiller COP depends only on the combination of PLRs and dry bulb temperatures in the absence of the mist system. This is because the heat rejection airflow required to maintain head pressure control is unique for a given combination of PLR and dry bulb temperature. While the chiller operated with the mist system, the heat rejection airflow interacted with not only the dry bulb temperature but also the moisture content which could vary independently with each other. This results in various degrees of the COP improvement for a given PLR. Regarding the

Table 2
Frequency distribution of relative humidity (RH) at different dry bulb temperatures (T_{db})

RH (%)	Dry bulb temperature (T_{db}) (°C)														Sub-total
	8–10	10–12	12–14	14–16	16–18	18–20	20–22	22–24	24–26	26–28	28–30	30–32	32–34	34–36	
90–100	0	0	169	312	515	575	440	498	907	904	335	4	0	0	4659
80–90	16	28	130	275	334	975	1386	632	807	1287	1503	440	0	0	7813
70–80	3	34	55	191	279	446	878	1123	463	480	897	984	434	0	6267
60–70	0	4	38	89	158	233	186	217	281	111	45	173	437	204	2176
50–60	0	0	28	4	48	89	95	68	33	29	0	9	29	52	484
40–50	0	0	0	0	0	0	21	33	20	1	0	0	0	0	75
30–40	0	0	0	0	0	0	0	0	7	0	0	0	0	0	7
Sub-total	19	66	420	871	1334	2318	3006	2571	2518	2812	2780	1610	900	256	21481

Data were collected at 15-minute intervals.

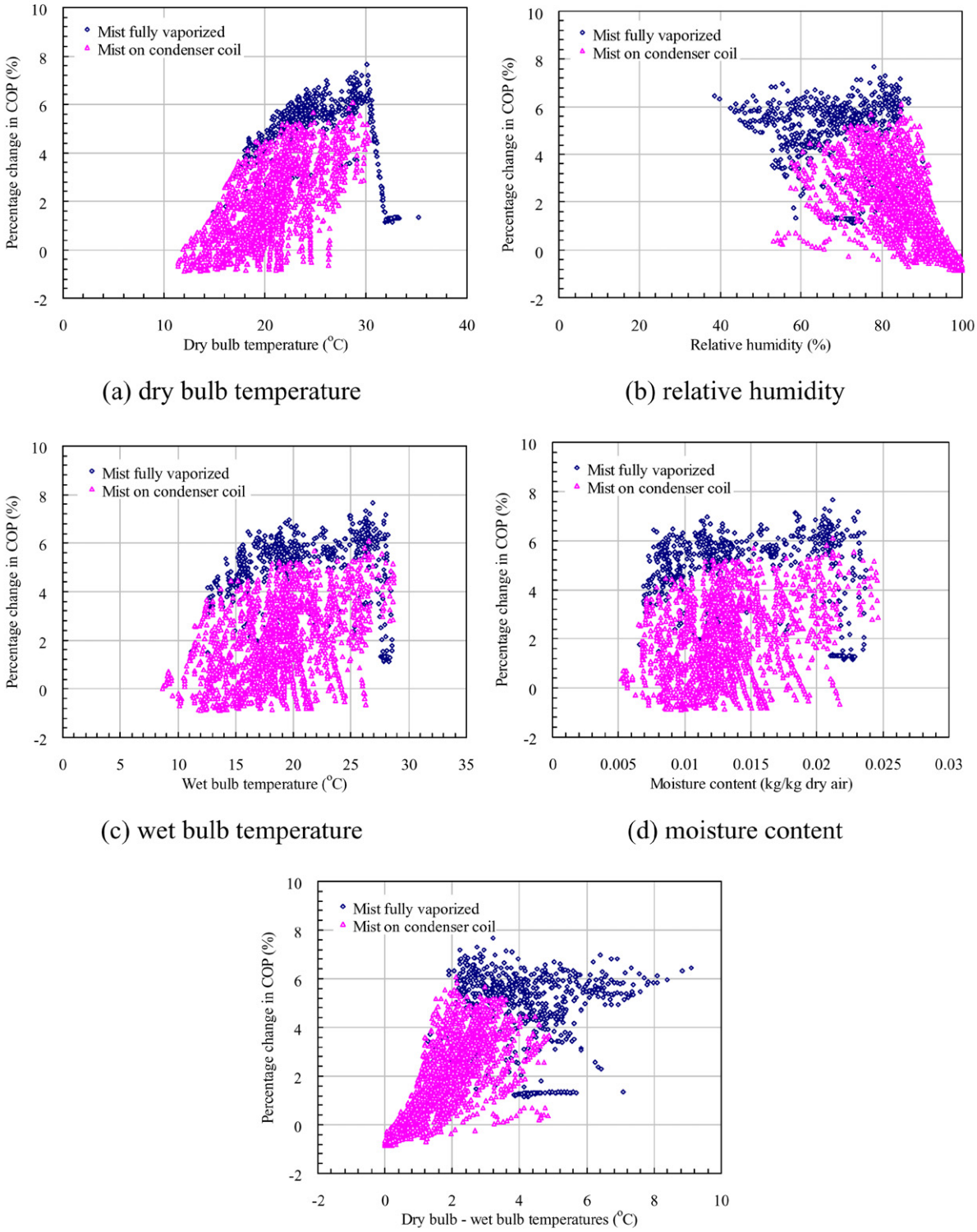

Fig. 4. Percentage change of chiller COP at part load ratios of 0.5–0.6 against different weather parameters.

two PLR ranges, the extent to which the COP can increase is different, though the spreads of the data are similar in some way with respect to each weather parameter. When the mist system was applied, the COP could increase more noticeably at lower PLRs than at near full load. This is because at lower chiller loads, the degree of modulating the heat rejection airflow is much higher when not all condenser fans are switched on under HPC. At near full load with the operation of all con-

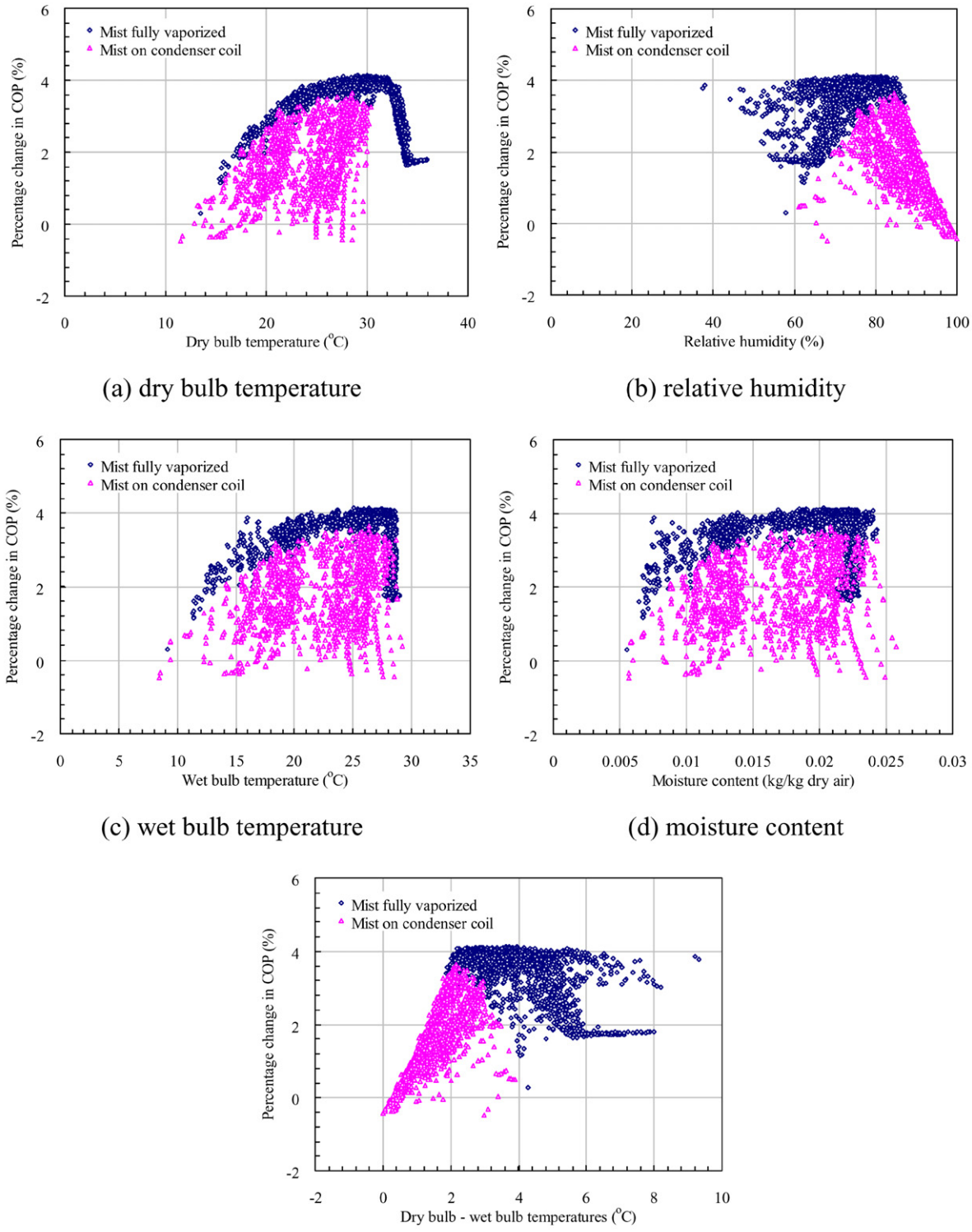

Fig. 5. Percentage change of chiller COP at part load ratios of 0.9–1 against different weather parameters.

denser fans, the increase of chiller COP depends mainly on a reduction in the condenser air temperature which is limited by the relative humidity of outdoor air.

The chiller COP could increase in varying degrees by up to 7.7% for 92.1% of the total operating time in the period of January to August 2007, though it could drop from baseline by up to 1.3% for 7.9% of the total operating time. The reduction of the chiller COP was always associated with the excessive mist carried over the condenser coil without undergoing vaporization by the condenser air stream. The reduced COP, indeed, is

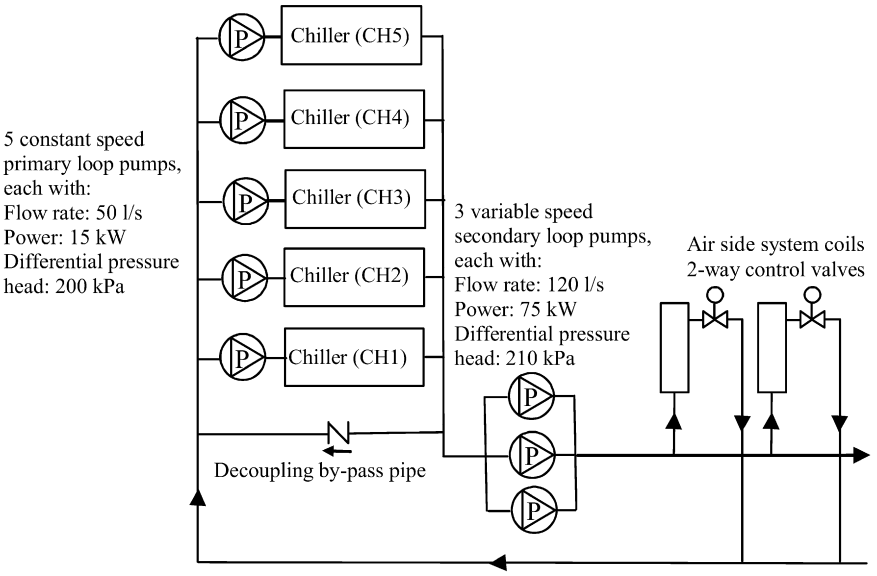

Fig. 6. Schematic of the chiller system.

due to the extra pump power while evaporative cooling has little or no effect on the decrease in the condenser air temperature because of the minimal difference between the dry bulb and wet bulb temperatures. It is possible to ensure a definite increase of chiller COP when mist pre-cooling was applied at RH $< 65\%$ or $(T_{db} - T_{wb}) > 3.2\,^{\circ}C$. Yet these two criteria screen out many operating conditions according to the frequency distribution of T_{db} and RH shown in Table 2 and the increase of COP would not be realized for 96.4% of the total operating time for RH $< 65\%$ and 73.5% of the total operating time for $(T_{db} - T_{wb}) > 3.2\,^{\circ}C$. On the other hand, the absolute increase of chiller COP was guaranteed when all the mist generated was fully vaporized by the ambient air before entering the condenser. Furthermore, the percentage increase of COP appeared to be higher in the perfect vaporization process. Yet no single or composite weather parameters was found to be suitable for illustrating the complete vaporization process for any given operating condition, with regard to the provision of the fixed mist generation rate for each of the refrigeration circuits activated.

4. Potential benefits from using mist pre-cooling

An assessment was made on the potential electricity savings by using mist pre-cooling based on the cooling load profile of an existing chiller plant serving an institutional building. Fig. 6 gives the arrangement of the chiller plant. It contains five identical air-cooled screw chillers equipped with mist systems as described in Section 3, each of the chillers is dedicated with one constant speed chilled water pump to maintain a fixed chilled water flow rate passing through it when operating. The determination of the electricity consumption of the primary loop pumps is based on their rate power and the number of chillers operating. For a given building cooling load, the flow rate of chilled water required at the secondary loop was identified from measurements and the least number of secondary loop pumps operated at equal flow to meet this flow rate. The electricity consumption of the secondary loop pumps was then determined based on their rated power and the cubic relationship between the power and flow. To meet the changing building cooling load, conventional chiller sequencing was implemented so all the chillers are operating at the same load, and no additional chillers start to operate until each of the running chillers is operating at full load. That means two, three, four and five chillers were operating when the system cooling load exceeded 1152, 2304, 3456 and 4612 kW, respectively. The load which each operating chiller carried was determined accordingly.

The building load profile refers a total set of 21481 data on the building cooling load and the coincident dry bulb temperature and relative humidity measured at 15-min intervals over the period of January to August 2007. Each of the load data was computed directly by the flow rate and temperatures of chilled water measured at the supply and return headers of the secondary chilled water loop. Table 3 represents the frequency distribution of the building cooling loads expressed as ratios (BLR) to the peak level of 4928 kW in various dry bulb temperature bins. The total cooling energy was 3,005,797 kWh over the period studied. Lower building load ratios appeared to scatter over a wide range of dry bulb temperatures. Data of higher building load ratios were generally gathered at higher outdoor temperatures with a narrower range. The building load ratios are 0.5 or below for 75.5% of the total operating time. Based on conventional chiller sequencing, the percentages of the total operating time in which one, two, three, four and five chillers running were 48.64, 23.53, 24.84, 2.97 and 0.02%, respectively.

Following the analysis on the percentage change of chiller COP with mist pre-cooling, some weather parameter settings may be applied to filter out certain operating conditions in which the unfavorable use of mist systems caused a decrease in the COP. Six cases described below were considered when calculating the total electricity consumption of the chillers operating for the building load profile. Case 1 (C1) refers to the base case where the mist system was idle (switched "OFF") all

Table 3
Frequency distribution of building cooling load data in different dry bulb temperature bins

BLR	Dry bulb temperature (T_{db}) (°C)														Sub-total
	8–10	10–12	12–14	14–16	16–18	18–20	20–22	22–24	24–26	26–28	28–30	30–32	32–34	34–36	
0.9–1	0	0	0	0	0	0	0	0	0	0	3	0	0	0	3
0.8–0.9	0	0	0	0	0	0	0	1	7	34	21	9	1	0	73
0.7–0.8	0	0	0	0	3	4	3	20	70	118	167	118	75	5	583
0.6–0.7	0	0	0	5	3	14	45	42	156	322	554	447	494	160	2242
0.5–0.6	0	0	1	6	27	98	158	124	216	383	555	499	200	86	2353
0.4–0.5	0	0	2	7	66	198	284	258	246	305	412	254	68	3	2103
0.3–0.4	0	0	13	16	110	174	367	446	303	232	318	105	18	1	2103
0.2–0.3	0	5	29	82	204	387	541	601	392	386	270	94	43	1	3035
0.1–0.2	5	15	183	420	453	949	1244	903	1054	990	468	76	0	0	6760
0–0.1	14	46	192	335	468	494	364	176	74	42	12	8	1	0	2226
Sub-total	19	66	420	871	1334	2318	3006	2571	2518	2812	2780	1610	900	256	21481

Data were collected at 15-minute intervals.

Table 4
Electricity consumption of chillers at different operating schedules of mist system

Case	C1	C2	C3	C4	C5	C6
Chiller consumption (kWh)	2,664,629	2,587,451	2,587,739	2,645,923	2,630,835	2,661,959
% saving from C1	–	2.90	2.89	0.70	1.27	0.10
% of total time with mist pre-cooling	0	92.1	100	11.4	26.5	3.6
% of total time with chiller energy savings	–	92.1	92.1	11.4	26.5	3.6
% of total time with extra chiller energy use	–	–	7.9	–	–	–

the time for each chiller operating. Cases 2 to 6 refer to different strategies for switching "ON" the mist system for each chiller operating: (C2) "ON" only when the COP could increase—virtual optimum control; (C3) "ON" all the time even when the COP dropped from the base case; (C4) "ON" only when the dry bulb temperature was higher than 28 °C at a relative humidity of less than 77%—adopted by the mist system supplier; (C5) "ON" only when the difference between the dry bulb and wet bulb temperatures ($T_{db} - T_{wb}$) exceeded 3.2 °C; (C6) "ON" only when the relative humidity was below 65%.

The total electricity consumption was calculated to be 144,210 kWh for the primary loop pumps and 196,958 kWh for the secondary loop pumps for all the cases where the same schedule of staging chillers was applied. It is noted that the overall electricity consumption of the pumps accounts for 11.4% of the electricity consumption of the chiller plant, with regard to the base case with the total electricity consumption of 2,664,629 kWh taken up by the chillers. Table 4 shows the annual electricity consumption of the chillers under different cases. Optimizing the operation of the mist systems enables the total electricity consumption of the chillers to drop by 2.9% or 77,178 kWh. However, it is difficult to implement the optimum mist control based directly on any ambient and load conditions. It is interesting to note that near optimal mist control can be achieved simply by interlocking the operation of the mist generating pumps and the chillers, as in case 3. The unfavorable mist generation resulted in an increase of 0.01% or 288 kWh only in the total chiller electricity consumption. It seems unwise to use some weather parameter settings to limit the unfavorable mist generation, based on the relatively small chiller energy savings in cases 4 to 6. Indeed, the limited operation of the mist systems brings very little chance to increase the chiller COP by mist pre-cooling in many operating conditions.

It is possible to assess the economic benefit of implementing mist pre-cooling in relation to the resultant electricity savings of 76,890 kWh in case 3 with a small degree of COP improvements. Considering an electricity tariff of HK$ 1 per kWh, the electricity cost savings of the chiller plant is HK$ 76,890 over the 8-month period. Assuming that the total capital cost is HK$ 150,000 for installing all the five chillers with mist installations, the simple payback period would be shorter than 2 years, suggesting that it is economically viable to consider mist pre-cooling as a standard energy saving measure for air-cooled chillers.

Based on the results in Table 4, more chiller energy use can be reduced when the mist systems run longer, suggesting that the mist systems should operate in line with the chillers in order to achieve maximum energy savings. The advantage and potential of applying mist pre-cooling have been fully realized for air-cooled chillers operating under subtropical regions. It is envisaged that energy savings from mist pre-cooling would be more significant if the chillers operate in a hot and arid environment in which the difference between the dry bulb and wet bulb temperatures is much higher.

5. Challenges of using mist per-cooling

It is possible to retrofit a mist system for any kind of air-cooled chiller system, regarding its simple design and installation and its independence with sequencing control of chillers and pumps. The present simulation analysis confirms that it is economically viable to consider mist pre-cooling as a standard energy saving measure for air-cooled chillers working even un-

der HPC with a low COP at part load operation. As far as energy saving is concerned, it is desirable to implement mist pre-cooling for all the operating time of chillers. Yet for many of the operating time mist could be carried over the condenser fins and coil as shown in Figs. 4 and 5, due to the excessive mist generation and incomplete vaporization by the condenser air. It remains to be investigated whether scaling and corrosion will be accelerated on the condenser fins and coil in a persistent damp environment. More research and survey should be done on what coating or special treatment on the heat transfer surfaces may be required to cope with the wet environment and on how proper maintenance practice should be developed to ensure the heat transfer effectiveness of air-cooled condensers with mist pre-cooling.

It is theoretically sound, but may not be practical, to adjust the mist generation rate in response to various ambient and chiller load conditions in order to avoid excessive mist which causes damping to the condenser fins and coil and even a reduction in the chiller COP. With regard to the pumps operating at high pressure and low flow, the possible means to adjust the mist generation rate rests on switching them on and off. A step adjustment on the mist generation rate may be feasible by installing multiple sets of water mist installations for a chiller. Yet it seems difficult to determine the required rate as surplus mist on the condenser coil means incomplete vaporization but still brings an increase in the COP for many operating conditions. Furthermore, no explicit indicator is available to judge if the actual rate matches with the required rate. Frequent switching of the pumps for adjusting the mist generation rate could accelerate the wear and tear problem. More importantly, the intermittent variation of the mist generation rate can cause a fluctuation in the reduced condenser air temperature, which in turn disturbs the stability of the condenser fans staged to deliver the heat rejection airflow required for controlling the condensing temperature at its set point. Although near-optimum performance can be achieved simply by interlocking the operation of the chillers and mist systems, it may still be worth considering precise control of mist generation rate with regard to the concern over the wet condenser conditions and to the possible change of air dryness under various climatic conditions.

This analysis indicates that mist pre-cooling helps boost a small increase of COP for chillers operating under HPC. Given the interaction between the mist generation rate, the heat rejection airflow required and the extent of reduction in the condenser air temperature, it is worth investigating how the use of mist pre-cooling can complement CTC to further enhance the COP of air-cooled chillers. Unlike HPC under which the heat rejection airflow tends to drop in response to the reduced chiller loads or ambient temperatures, the heat rejection airflow under CTC is generally kept at its maximum level in many operating conditions. The full vaporization process of mist can occur more often under operating conditions with the maximum heat rejection airflow. This suggests that mist pre-cooling can be used more effectively to increase the chiller COP. Due to the gentler change of the heat rejection airflow under CTC at various operating conditions, there should be less demanding on the fine adjustment of mist generation rate. It is speculated that a definite advantage with optimum energy savings can be achieved from the simple interlocking operation of mist systems and chillers under CTC. Detailed analysis on integrating mist pre-cooling with CTC will be the future research work in order to learn better the ultimate improvement in the COP of air-cooled chillers.

6. Conclusions

This paper investigates how mist pre-cooling helps improve the energy performance of air-cooled chillers. The advantage of this application rests on the decrease of compressor power when the dry bulb temperature of air entering the condenser drops to approach its wet bulb by mist vaporization with insignificant consumption of water and pump power associated with the mist generation. A simple regression-based model was developed to simulate the part-load and off-design performance of an existing chiller with mist installations. The use of mist pre-cooling could increase the COP in various degrees by up to 7.7%, with regard to an air-cooled screw chiller operating under HPC in subtropical regions. Yet up to a 1.3% reduction in the COP could result from the extra pump power with excessive mist generation when the evaporative cooling has little or no effect on the decrease in the condenser air temperature because of the minimal difference between the dry bulb and wet bulb temperatures.

Regarding the greatest percentage uncertainty of 1.93% in the chiller COP computed from the temperature and power variables with their own measurement errors, the increase of chiller COP can be distinguishable when its percentage change is above 1.93% which accounts for 66.7% of the total operating time. In cases where the percentage increase of chiller COP is less than 1.93%, the energy savings brought from mist pre-cooling can be identified more directly by noting a reduction in the chiller power measured with an error of 0.09% at most. Although mist pre-cooling could bring about a savings of 2.9% only in the total chiller electricity consumption, its economic benefit was verified based on a simple payback period of shorter than 2 years. It is envisaged the COP improvements made by mist pre-cooling would be more considerable for chillers operating under CTC or under the hot and arid environment with a large difference between the dry bulb and wet bulb temperatures.

It is simple and easy to design and install a mist system for any given air-cooled chiller system. A straightforward means to maximize electricity savings is to operate the mist system continuously with the on-line chiller, regardless of ambient and load conditions. The interlocking operation of the chiller and mist system is free of control inaccuracy associated with the measurement error of the temperature and power variables. Yet the major challenges of operating a mist system may involve identifying the potential impacts on the wet condenser conditions resulting from unavoidable excessive mist generation and assessing the importance of the precise adjustment of mist generation rate in response to various operating conditions. These should be addressed in order to foster mist pre-cooling as a

standard energy efficient measure for air-cooled chillers and constitute the future research work.

Acknowledgements

The work described in this paper was supported by a grant from the central research grant of The Hong Kong Polytechnic University, Project A/C Code: G-U272. The authors would like to thank staff of the Facilities Management Office, The Hong Kong Polytechnic University, for their help with the collection of chiller operating data.

References

[1] K.A. Brownell, S.A. Klein, D.T. Reindl, Refrigeration system malfunction, ASHRAE Journal 41 (2) (1999) 40–46.
[2] K.A. Manske, D.T. Reindl, S.A. Klein, Evaporative condenser control in industrial refrigeration systems, International Journal of Refrigeration 24 (2001) 676–691.
[3] R.J. Love, D.J. Cleland, I. Merts, B. Eaton, What is the optimum compressor discharge pressure set point for condensers? EcoLibrium (August 2005) 24–29.
[4] M.A. Roper, Energy efficient chiller control, Technical note TN 16/2000, Building Services Research and Information Association, Bracknell, 2000.
[5] M. Smith, G. King, Energy saving controls for air-cooled water chillers, Building Services Journal (April 1998) 47–48.
[6] K.T. Chan, F.W. Yu, Applying condensing-temperature control in air-cooled reciprocating water chillers for energy efficiency, Applied Energy 72 (2002) 565–581.
[7] F.W. Yu, K.T. Chan, Optimizing condenser fan control for air-cooled centrifugal chillers, International Journal of Thermal Sciences 47 (7) (2008) 942–953.
[8] F.W. Yu, K.T. Chan, Advanced control of heat rejection airflow for improving the coefficient of performance of air-cooled chillers, Applied Thermal Engineering 26 (2006) 97–110.
[9] H. Zhang, S.J. You, H.X. Yang, J.L. Niu, Enhanced performance of air-cooled chillers using evaporative cooling, Building Services Engineering Research & Technology 21 (4) (2000) 213–217.
[10] G.J. Bom, R. Foster, E. Dijkstra, M. Tummers, Evaporative air-conditioning: applications for environmentally friendly cooling, World Bank Technical Paper No. 421. Energy Series, World Bank, Washington, DC, 1999.
[11] F.W. Yu, K.T. Chan, Application of direct evaporative coolers for improving the energy efficiency of air-cooled chillers, Journal of Solar Energy Engineering 127 (3) (2005) 430–433.
[12] Air-conditioning & Refrigeration Institute, Standard 550/590: Performance rating of water chilling packages using the vapour compression cycle, Air-conditioning & Refrigeration Institute, Arlington, Virginia, 2003.
[13] F.C. Winklemann et al., DOE-2 Supplement, Version 2.1E, Lawrence Berkeley National Laboratories, Berkeley, CA, 1993.